Heliyon 9 (2023) e21041

Contents lists available at ScienceDirect

Heliyon

journal homepage: www.cell.com/heliyon

Defining the optimal conditions using FFNNs and NARX neural networks for modelling the extraction of Sc from aqueous solution by Cryptand-2.2.1 and Cryptand-2.1.1

Ali Dawood Salman [a,b,*], Saja Mohsen Alardhi [c], Forat Yasir AlJaberi [d], Moayyed G. Jalhoom [c], Phuoc-Cuong Le [e], Shurooq Talib Al-Humairi [f], Mohammademad Adelikhah [g], Miklós Jakab [h], Gergely Farkas [i], Alaa Abdulhady Jaber [j]

[a] Sustainability Solutions Research Lab, University of Pannonia, Egyetem str. 10, H-8200 Veszprem, Hungary
[b] Department of Chemical and Petroleum Refining Engineering, College of Oil and Gas Engineering, Basra University for Oil and Gas, Iraq
[c] Nanotechnology and advanced material research center, University of Technology- Iraq
[d] Chemical Engineering Department, College of Engineering, Al-Muthanna University, Al-Muthanna, Iraq
[e] The University of Danang,University of Science and Technology, Danang 550000, Viet Nam
[f] Chemical Engineering department, University of Technology, Baghdad 10070, Iraq
[g] Institute of Radiochemistry and Radioecology, Research Centre for Biochemical, Environmental and Chemical Engineering, University of Pannonia, 8200 Veszprem, Hungary
[h] Department of Materials Engineering, Faculty of Engineering, University of Pannonia, 8201 Veszprém, Hungary
[i] Department of Organic Chemistry, Institute of Environmental Engineering, University of Pannonia, H-8201 Veszprém, P. O. Box 158, Hungary
[j] Mechanical Engineering Department, University of Technology - Iraq, Baghdad, Iraq

ARTICLE INFO

Keywords:
Molecular recognition
Scandium
Macrocyclic compounds
Artificial neural network
NARX model

ABSTRACT

The main aim of this study is to figure out how well cryptand-2.2.1 (C 2.2.1) and cryptand-2.1.1 (C 2.1.1) macrocyclic compounds (MCs) work as novel extractants for scandium (Sc) by using an artificial neural network (ANN) models in MATLAB software. Moreover, C2.2.1 and C2.1.1 have never been evaluated to recover Sc. The independent variables impacting the extraction process (concentration of MC, concentration of Sc, pH, and time), and a nonlinear autoregressive network with exogenous input (NARX) and feed-forward neural network (FFNN) models were used to estimate their optimum values. The greatest obstacle in the selective recovery process of the REEs is the similarity in their physicochemical properties, specifically their ionic radius. The recovery of Sc from the aqueous solution was experimentally evaluated, then the non-linear relationship between those parameters was predictively modeled using (NARX) and (FFNN). To confirm the extraction and stripping efficiency, an atomic absorption spectrophotometer (AAS) was employed. The results of the extraction investigations show that, for the best conditions of 0.008 mol/L MC concentration, 10 min of contact time, pH 2 of the aqueous solution, and 75 mg/L Sc initial concentration, respectively, the C 2.1.1 and C 2.2.1 extractants may reach 99 % of Sc extraction efficiency. Sc was recovered from a multi-element solution of scandium (Sc), yttrium (Y), and lanthanum (La) under these circumstances. Whereas, at a concentration of 0.3 mol/L of hydrochloric acid, the extraction of Sc was 99 %, as opposed to Y 10 % and La 7 %. The Levenberg-Marquardt training algorithm had the best training performance with an mean-

* Corresponding author. Sustainability Solutions Research Lab, University of Pannonia, Egyetem str. 10, H-8200 Veszprem, Hungary.
E-mail addresses: ali.dawood@buog.edu.iq, ali.dawood@mk.uni-pannon.hu (A. Dawood Salman).

https://doi.org/10.1016/j.heliyon.2023.e21041
Received 8 May 2023; Received in revised form 10 October 2023; Accepted 13 October 2023
Available online 19 October 2023

squared-error, MSE, of $5.232x10^{-6}$ and $6.1387x10^{-5}$ for C 2.2.1 and C 2.1.1 respectively. The optimized FFNN architecture of 4-10-1 was constructed for modeling recovery of Sc. The extraction process was well modeled by the FFNN with an R^2 of 0.999 for the two MC, indicating that the observed Sc recovery efficiency consistent with the predicted one.

1. Introduction

The metallurgical, chemical, and electrical industries can all benefit from the utilization of the rare earth element, scandium (Sc) [1,2]. Scandium has a smaller ion radius (0.745 Å) and lower hydroxide alkalinity than yttrium (0.9 Å) and lanthanum (0.98 Å) [3]. It has a substantially higher proclivity for both complexes generation and hydration. Scandium has attracted a lot of attention in recent years due to its unique features in solid oxide fuel cells, aluminum alloys, and other cutting-edge materials [4–8]. Scandium is frequently found in Sc-bearing ores alongside other rare earth elements, Ti, V, and U [7,9]. The majority of Sc is currently extracted as a by-product from waste of TiO_2, red mud, molten aluminum slag, tungsten slag, among other sources [8,10,11]. Sc content was determined to be less than 200 ppm. However, the majority of these resources are composed of other elements including Al, Fe, Ti, and Zr [12,13]. Because of the low Sc content, the recovery process must be highly selective for Sc. In this context, the majority of recovery research has concentrated on the hydrometallurgy process [14,15]. Leaching of Sc into the aqueous phase is the initial step. Then, to enhance and purify Sc from the leaching fluid, several separation procedures are used [16,17]. Solvent extraction (SX) is the most widely used for Sc recovery [10,18], but other methods, such as resin ion-exchange and polymer inclusion membrane, have also been investigated [19–22]. Acidic and neutral organophosphorus compounds, particularly Cyanex 272, tributyl phosphate (TBP), di-2-ethylhexyl phosphoric acid (D2EHPA), and P507, are extensively used as extractants for Sc in the SX process [9,23–26].

Macrobicyclic ligands, such as cryptand-2.2.1 (C2.2.1) and cryptand-2.1.1 (C2.1.1), are composed of two bridgehead atoms (N, C, P, and so on) linked by three bridges [27,28]. Their cage-like cavities can surround metal ions and create stable complexes, which are typically spherical [29–31]. Recently, we investigated the ability of some of MC compounds for Sc such as crown ethers (12-crown-4, 15-crown-6, DC-18-crown-6) and cryptands (cryptand-2.2.2, cryptand-2.2) [21,32,33].

The goal of this work was to provide a thorough analysis utilizing an optimization method that will address the key factors affecting the extraction of Sc ions from aqueous matrices employing unconventional MC extractants like cryptand-2.2.1 and cryptand-2.1.1. This paper aims to describe how to use cryptands as extractants to increase metal ion selectivity. The MCs used in the study, which has donors for both oxygen and nitrogen, acts as the bridgehead atom. The recovery of Sc from three elements model solution was then carried out based on optimization results to explore the selectivity of MC towards these trivalent ions. The neural network is the most common way to make predictive models that can be used to do nonlinear statistical modeling. However, the various experimental studies could not ascertain the extent of a non-linear relationship between the process variables such as pH, concentration of MCs (mol/L) and Sc (mg/L), contact time and extraction efficiency.

Machine learning is becoming a potent and popular technique for resolving a variety of issues [34–38].Neural networks (NNs) are effective of optimizing nonlinear systems and forecasting the production of new data sets, among other optimization applications. In recent years, NNs have been used as an effective modeling tool in a range of processes, including adsorption [39–43], flotation, SX, and a variety of other areas of mineral processing. Consequently, the greatest obstacles in the recovery of Sc from aqueous solution are its low concentration and low selectivity. This work proposed new extractants for Sc recovery in response to the challenges raised above. In this paper, attempts have been done to identify the ability and optimum conditions for Sc extraction process by MC (C2.2.1 and C2.1.1) using ANN technique. Moreover, applying these conditions to extract Sc from multi trivalent metal ions (M^{+3} = Sc, La, Y). To our knowledge, the recovery of Sc by C2.2.1 and C2.1.1 has never been investigated. The goal of this work is to extract Sc from aqueous solution using cryptand-2.2.1 (C 2.2.1) and cryptand-2.1.1 (C 2.1.1) macrocyclic compounds, using NARX, and FFNN techniques, and compare the accuracy and productivity of the model behaviour. This could be of a potential value in the separation and the purification of Sc in the REEs processing industry.

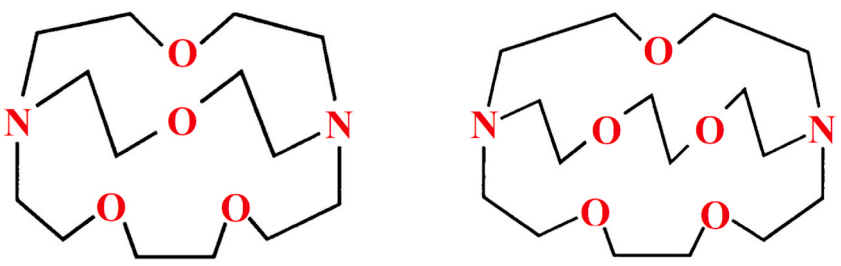

Fig. 1. Chemical structures of the C2.2.1 (a) and C2.1.1 (B) extractants.

2. Materials and methods

2.1. Materials

The analytical grade of all compounds allowed for their use without further purification. 4,7,13,16,21-pentaoxa-1,10-diazabicyclo [8.8.5]tricosane cryptand-2.2.1 ($C_{16}H_{32}N_2O_5$, 96 %), 4,7,13,18-tetraoxa-1,10-diazabicyclo[8.5.5]eicosane cryptand-2.1.1 ($C_{14}H_{28}N_2O_4$, 98 %). Fig. 1 shows their structures, which were sourced from Sigma-Aldrich Chemicals Co. 1,2-dichloroethane ($C_2H_4Cl_2$, 99.8 %), chloroacetic acid ($C_2H_3ClO_2$, 99 %) and chloroform ($CHCl_3$, 99 %) were purchased from Merck Chemicals Co., acetic acid (CH_3COOH, 20 % v/v), Ethanol (C_2H_5OH, 96 %),sodium hydroxide (NaOH, 97 %), hydrochloric acid (HCl, 37 %) and scandium solution (1 g/L) in diluted nitric acid (2 %) were purchased from VWR Chemicals BDH Co, Leuven, Belgium. Xylenol orange tetrasodium salt (96 %) was purchased from BDH Chemicals Ltd., Poole, England. All aqueous solutions were prepared with deionized water. Sc, Y, La standards.

2.2. Instrumentation and analytical procedures

The determination of REEs concentrations in aqueous solutions was carried out by atomic absorption spectrophotometer (AAS), Shimadzu AA-7000 type, Japan instrument. The pH of aqueous solutions that a pH meter has measured (METTLER TOLEDO, Seven Multi, Germany).

2.3. Artificial neural network model

The Artificial Neural Networks (ANNs) are computational models that replicate how the human brain learns and makes decisions [44–46]. Prior to use, they are designed to go through a learning process. The network structure, the type of activation functions in the neurons in human brain, the learning time, and the amount of neurons used throughout the learning process are just a few of the essential factors that have an impact on their capacity for decision-making and the accuracy of their conclusions. With over 40 years of use, the ANN is a proven technique for various forecasting issues in several fields. ANN appears to be an excellent option for representing non-linear dependency due to its universal approximation functional form [47,48].

The main objective of artificial neural networks is to establish a generalized, non-linear connectivity between input and output data sets. Input, output, and at least one hidden layer are often used to construct different types of ANNs. Fig. 2, describe the summary of main steps to find the optimum conditions for Sc recovery by MC.

The complexity of the link between the input and output data sets determines the number of hidden layers. In this study, a multilayer ANN known as a supervised feed-forward multilayer perceptron (MLP) was used. The MLP neural network is the most popular and straightforward ANN assigned to feed-forward neural network FFNNs model. A single input layer, one or more hidden layers, and a single output layer are all part of the numerous layers that make up FFNNs. Information can only advance to the output layer due to the connection arrangements between the layers [44,49]. $X_1, X_2, \ldots\ldots, X_n$; refers to the network's input, the output of the hidden and output layers is denoted by the letters O and Y. However, weight matrices can be used to indicate the relationship between the input and hidden layers as well as the hidden and output data as W_{ij} and W_{jk}, respectively [50]. Let l, n, and k refer to the number of neurons in the input, hidden, and output layers in order to determine the desired data, respectively:

$$O_j = f\left[\sum_{i=1}^{n} W_{ij}X_i + b_j\right] \text{ for j} = 1, 2, \ldots\ldots, 1 \quad (1)$$

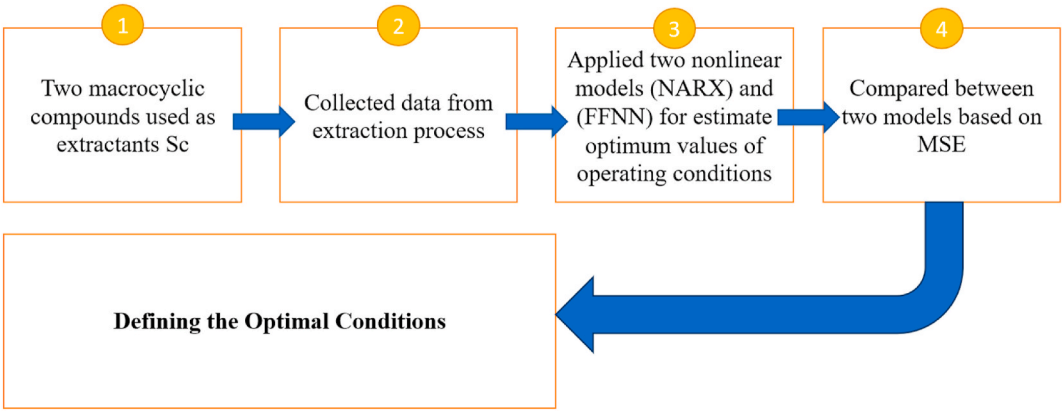

Fig. 2. Summary of main steps to find the optimum conditions for Sc recovery.

$$Y_k = f\left[\sum_{j=1}^{l} W_{jk} O_j + b_k\right] \text{ for k} = 1, 2, \ldots\ldots, l \tag{2}$$

where b_j and b_k stand for the threshold factors for the neurons in the hidden and output layers, respectively, and f is the activation function. The input, hidden, and output layers of the appropriate MLP are included in this study. However, the parameters in the input data set and what is needed to obtain from the network determine how the neurons in the input and output layers function.

The network in this case comprises four inputs: MCs compounds, pH, contact time, and the concentration of Sc. The output is the recovery of Sc. On the other hand, the number of neurons in the buried layer is affected through trial and error methods. It should be noted that the applied activation function uses linear activation functions for the input and output layers while claiming non-linear activation functions for the hidden levels. The following equation is used in the hidden layer [51]:

$$f(x) = \frac{1}{1 + e^{-x}} \tag{3}$$

The forward propagation of the input data is done in order to apply the ANN. Then, to calculate the square error value, E, equation (4) is used [52]. In this equation, *Yk* and *Fk* refer to the predicted and expected output, respectively. After back-propagating the incorrect value, the gradient descent method is used to rectify the weights between the layers.

$$E = \frac{1}{2}\sum_{k=1}^{l} (F_k - Y_k)^2 \tag{4}$$

The nonlinear autoregressive, NARX neural network has a number of layers, an output feedback connection, and is a nonlinear autoregressive network with an exogenous input [53]. The NARX neural network employs an iterative training method in which the biases and weights are incrementally changed to improve the model performance at each stage. As long as they are available, the network's outputs are regressed with the target of the actual values during training, and the results are sent back to the network.

Compared to other networks, NARX models provide an additional degree of flexibility when incorporating information from exogenous inputs. The model's accuracy is increased, and the number of parameters needed is reduced owing to the additional degree of freedom. Equation (5) shows the NARX outputs during training [54].

$$y(t) = f\left[u(t - n_u), \ldots u(t-1), u(t), y(t - n_y), \ldots. \; y(t-1)\right] \tag{5}$$

where:

The non-linear function is called *f*.

The network input at time t is *u(t)*.

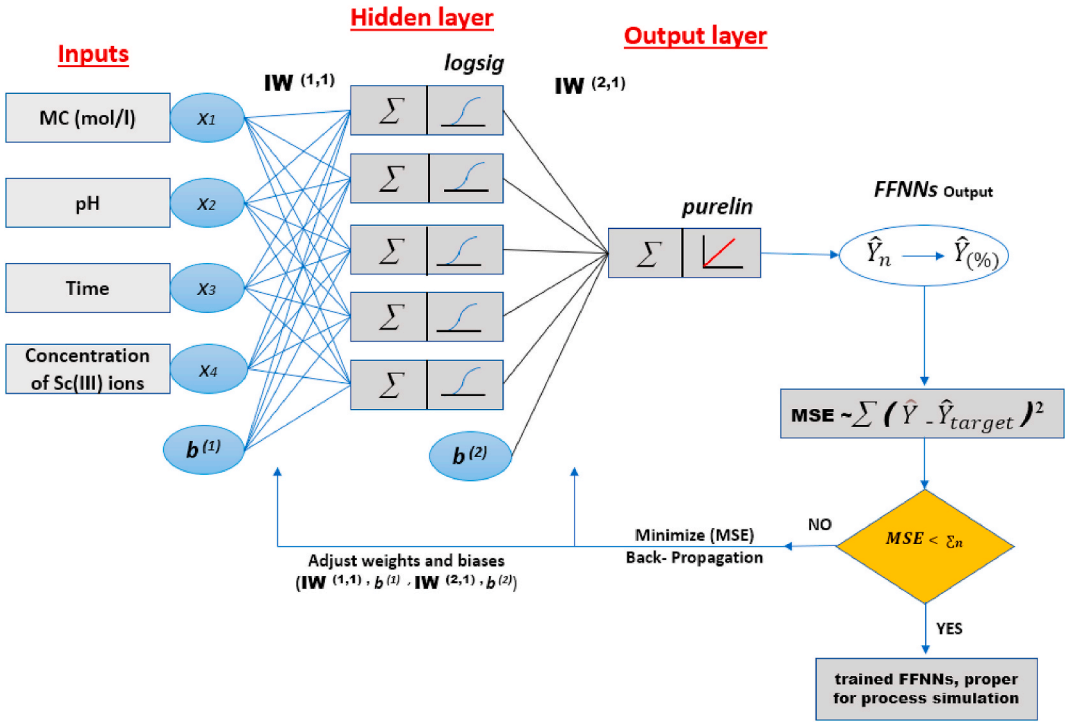

Fig. 3. Feed-forward neural networks, FFNNs, topology developed to predict the efficiency of the Sc extraction process.

The network output at time t is denoted by $y(t)$.

The input and output are in the following order: n_u and n_y.

When multi-layer perception is incorporated into the f method, the resulting system is referred to as the NARX network [39].

Two indicators were used in this study to evaluate the NARX and FFNN models using the predicted and actual results to check the reliability of the NARX and FFNN models. These indicators are mean-squared-error, MSE and extraction efficiency, E%.

$$MSE = \frac{1}{n}\sum_{i=1}^{n}\left(D_a(t) - D_f(t)\right)^2 \tag{6}$$

$$RE = \frac{D_a(t) - D_f(t)}{D_a(t)} \times 100 \tag{7}$$

where:

$D_f(t)$ denotes the predicated value, while $D_a(t)$ is the actual value at time t.

The criteria employed to assess model performance were MSE and RE. Utilizing several indicators served to verify the model's accuracy. By analysing the error between the actual and anticipated results, all indicators were based on the results that were attained.

2.3.1. Methodology of FFNNs and NARX models design

Fig. 3 depicts the topology of the generated network FFNNs [4:10:1] by directly illustrating the connections between inputs and artificial neurons. The network was trained by modifying the model parameters (weights and biases) to minimize the mean-squared-error (MSE), as shown in Fig. 2. In other words, the smaller MSE will lead to the greater the network's prediction ability. The input nodes used for training are 4 (MCs type compound, pH, time, Sc concentration), the hidden neurons are 10, and the output node is 1 (extraction efficiency).

To construct a suitable FFNNs, the back-propagation training process was applied using the MATLAB neural network toolbox. The weights were randomize initialized to begin the training process. After feeding the input layer, the input variables (MC concentration, pH, contact time, and Sc concentration) were multiplied by the first weight matrix and transferred to the hidden layer (Wij). The output vector of the hidden layer is created by adding the values that result from the multiplication step and passing them through the Sigmoid activation function in the hidden layer neurons. This vector is multiplied by the four weights matrix (W_{jk}) and sent to the output layer in order to predict the objective function, extraction efficiency percent of Sc. The error value is then determined by comparing the target and expected patterns.

Otherwise, the error is propagated backward to update the weights using an appropriate training technique, such as the Quasi-Newton algorithm, Levenberg-Marquardt algorithm, etc. The training will be terminated if the error is within the stated limit. The steps above are continued until the error falls within the desired range or the set number of iterations has been reached. After the network has been properly trained, it must be tested using data that has never been seen before for validation purposes. Several FFNNs

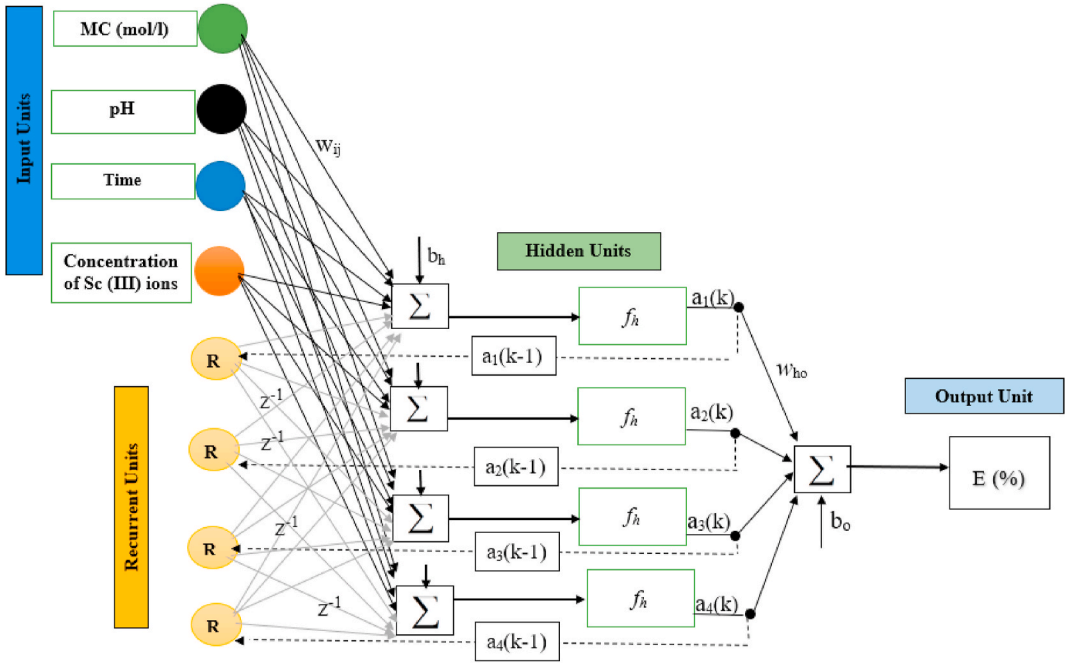

Fig. 4. Nonlinear autoregressive neural network NARX model structure of Sc extraction process.

models were evaluated in this study. Each model included a varying number of hidden layers and a varied number of neurons. Additionally, various training procedures were evaluated and compared in terms of MSE and correlation factor. Two techniques were used to evaluate model performance: mean MSE and coefficient of determination (R^2). A more accurate estimation of extraction efficiency was achieved by using an FFNNs model with a higher R^2 and lower MSE.

Fig. 4 shows the two layers of NARX that were employed in this study to forecast the extraction efficiency (E%) of macrocyclic chemicals. Time, dosage, pH, and initial concentration are the four inputs that make up the network's input layer. There is also one output layer (E%). Fig. 3 shows the network bias (b_h), network weight (w_{ij}), and delay element (z).

2.4. Methodology of NARX model design

1 the weights and biases of NARX network are randomly chosen.
2 the activation functions for hidden and output layers are set by default to hyperbolic tangent function (tansig) and linear function (purelin) in most network training, respectively.
3 the network is prone to the local optimization, resulting in a poorly performing training result, Therefore, algorithms of optimization, characterized are often used to optimize the connection weights and biases of BP neural network, and obtain better model prediction performance (iteration).
4 stop iteration at optimal transfer function, weights and biases.
5 training network.
6 updating weights and biases.
7 prediction results.

For NARX network modelling, 60 points datasets (30 points were input two times for training, each point has 4 different parameters) were used as input. The creation of a NARX neural network involves a number of phases, including gathering the experimental data needed for network testing, validation, and training. Before moving on to the testing session, which was based on unseen data input, the training and validation data set was created in a parallel session to train and validate the model. MATLAB R2021a was used and trainlm function was chosen for network training; many configurations were tested in this work to identify the most effective network topology. The ideal network topology that was utilized to build the model consisted of three hidden layers, each with 10 neurons, one input layer with 4 nodes, and one output layer with 1 node. The network transfer function chosen was the tansig function.

2.4.1. Optimization the best condition of artificial neutral network models

To optimize the performance of the ANN design for simulating the extraction of Sc, the hidden neurons were adjusted using the

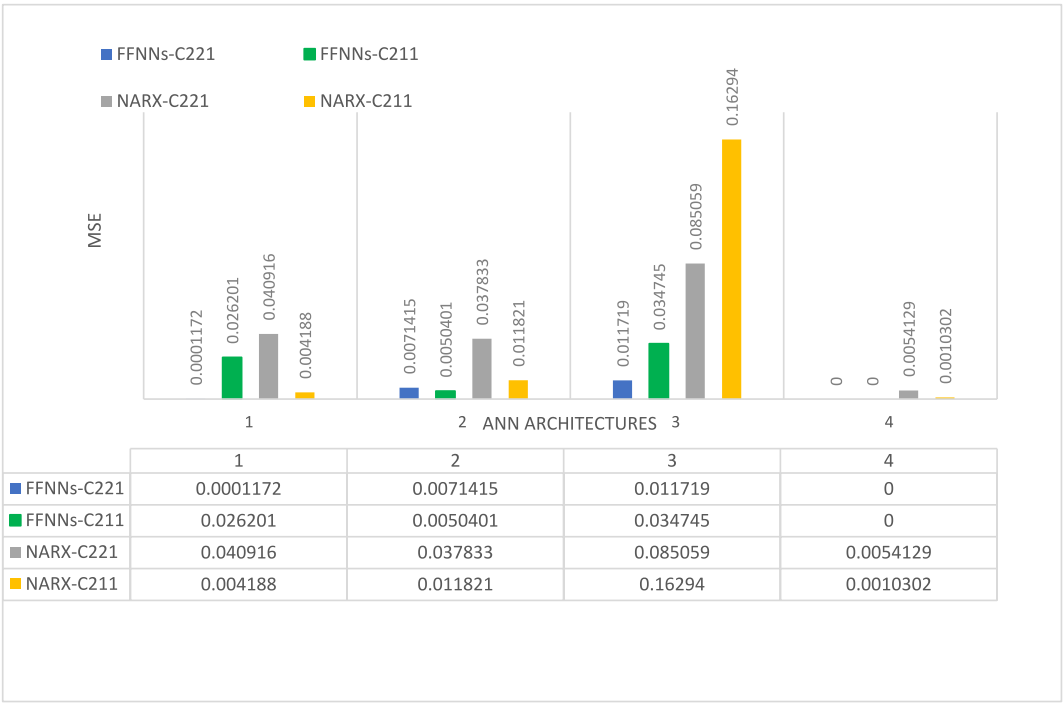

	1	2	3	4
FFNNs-C221	0.0001172	0.0071415	0.011719	0
FFNNs-C211	0.026201	0.0050401	0.034745	0
NARX-C221	0.040916	0.037833	0.085059	0.0054129
NARX-C211	0.004188	0.011821	0.16294	0.0010302

Fig. 5. Optimization of the training function, number of layers, and the hidden neurons of each of the ANN architecture used for modeling the extraction of Sc.

chain rule. According to the chain rule, the least amount of network error is produced by an optimized ANN model. In order to find the configuration with the lowest error and highest R^2 during network training, the hidden neurons of the networks were changed from 3 to 10 for each trial. For each trial, four different network configurations were tested. The training, validation, and testing were all improved as a result.

Fig. 5 illustrates the specifics of the Sc recovery optimization that was examined in this work. The network error measured by MSE for the FFNNs and NARX is impacted by the variance in the hidden neurons. Table 1 shows the details of the parameter estimation for each trial based on the training function, number of layers, and number of hidden neuron optimization. With hidden neurons equal to 10, optimized ANN architecture of 4-10-1 was constructed for modeling recovery of Sc as shown in Fig. 6 (a and b). In the current investigation, input and output parameters were supplied into a network. Table 1 shows the parameters' ranges.

2.4.2. The limitations of ANN are

- The neural network required training to operate.
- The structure of a neural network is disparate from the structure of microprocessors therefore required to be emulated.
- It needed high processing time for big neural networks.
- Fixed sized inputs: A neural network architecture has a fixed number of input layers. As such, it can only take a fixed sized input and output for any task. This is a limiting factor for many patterns recognition tasks.

This limitation can be improved.

1. Increase hidden Layers.
2. Change Activation function.
3. Change Activation function in Output layer.
4. Increase number of neurons.
5. Weight initialization.
6. More data.
7. Normalizing/Scaling data.
8. Change learning algorithm parameters.

The complexity of algorithms: there are 4 factors to consider here i.e. iterations, layers, nodes in each layer and training examples. Table 2 compare the complexity of the proposed models.

2.5. Determining the parameters of the process

At room temperature of 25 °C, recovery experiments with two different macrocyclic chemical types, C 2.2.1 and C 2.1.1, were performed. An extensive study was conducted to identify which variables most significantly influenced recovery process. As shown in Table 3, the four independent variables that chosen for the optimization process were the concentration of C 2.2.1 and C 2.1.1 in mol/L, the concentration of Sc in mg/L, pH, and time in minutes. The multielement extraction was carried out after determining the best Sc recovery conditions and analyzing the interaction of all variables.

2.6. Solvent extraction of Sc from model solution and its recovery from organic phase

The methods for extracting Sc covered in the optimization study were as follows: equal volumes (10 mL) of the aqueous phase (Sc solutions) and organic phase (1,2 dichloroethane contained C2.2.1 or C2.1.1) were contacted and combined in the separatory funnel. It is preferable to combine the organic phase with distilled water prior to the extraction process to achieve saturation with the aqueous phase. The organic and aqueous phases were separated after stabilizing the phases, and the aqueous phase was assessed using an AAS apparatus to confirm the Sc content and guarantee total accuracy.

The Sc ions were found in the separated organic phase as complexes with C2.2.1 or C2.1.1, and the recovery of Sc was the goal in the next stage. Under the following conditions: 0.008 mol/L C2.2.1 and C2.1.1, 25 mg/L Sc, La, and Y, 10 min of extraction time, varied pH

Table 1
Optimization of the training function, number of layers, and the hidden neurons of each architecture used to model the extraction of Sc by C2.2.1 and C2.1.1.

No.	Training function	No of layers	No of neurons	FFNNs		NARX		Architecture of network
				MSE for macrocyclic compounds				
				C221	C211	C221	C211	
1	trainlm	2	3	0.0001172	0.026201	0.040916	0.004188	4-3-1
2	trainbfg	2	4	0.0071415	0.0050401	0.037833	0.011821	4-4-1
3	trainr	3	4	0.011719	0.034745	0.085059	0.16294	4-4-1
4	trainlm	2	10	$5.232*10^{-6}$	$6.1387*10^{-5}$	0.0054129	0.0010302	4-10-1

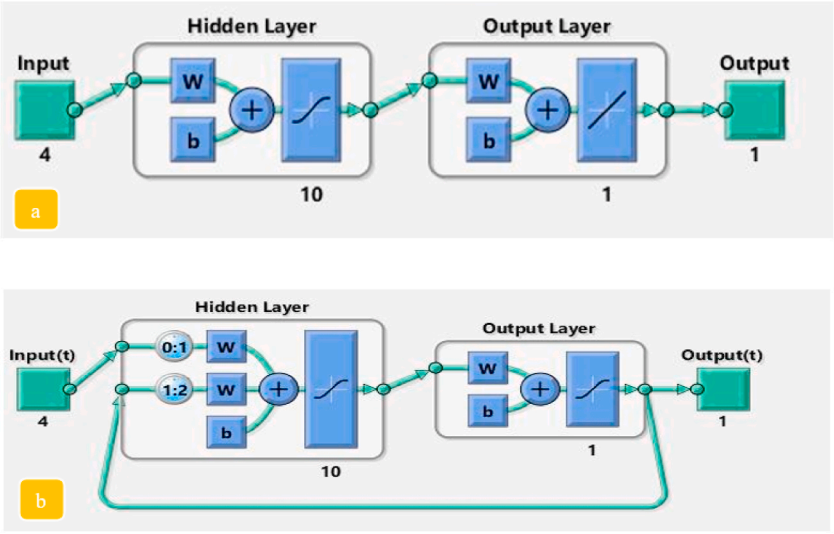

Fig. 6. Architecture of selected network for prediction the extraction of Sc for C2.2.1 and C2.1.1:(a) FFNNs and (b) NARX.

Table 2
the comparison of complexity of the proposed models.

No	Neural Networks (NN)	Machine Learning models (ML)
1	NN is a collection of machine learning methods for modeling data with graphs of neurons.	Advanced algorithms are used by machine learning to analyze data, learn from it, and apply those learnings to find interesting and relevant patterns.
2	Neural networks do not need human interaction since the stacked layers within convey the data via hierarchies of different concepts, eventually making them capable of learning from their mistakes. NN arranges algorithms in a way that it can make accurate decisions on its own.	Although machine learning models can learn from data, in the beginning they may need some human interaction. Machine learning models make judgments based on what they have learnt from the data.
3	There are four different types of neural networks: feed-forward, recurrent, convolutional, and modular.	There are two categories of machine learning models: supervised learning models and unsupervised learning models.
4	A neural network's structure is very intricate. It involves a system of interconnected nodes arranged in layers, each of which classifies the features and data from the layer before it transmits the classification to the nodes in the layer below.	A neural network's structure is very intricate. It involves a system of interconnected nodes arranged in layers, each of which classifies the features and data from the layer before it transmits the classification to the nodes in the layer below.

Table 3
Experimental range and levels of variables used in the ANN models.

Type	Variables	Range	Number of variables
Inputs	MC (mol/L)	0.002-0.010 (step 0.002)	5
	pH	1-5 (step 1)	5
	Time (min)	3-15 (step 3)	5
	Concentration of Sc	25-125 (step 25)	5
Outputs	Extraction efficiency % of Sc	4.7–99.0 for C2.2.15.0–99.3 for C2.1.1	18
			22

solutions, and a 1: 1 organic to aqueous phase (O/A) ratio, Sc was extracted from synthetic multi metal ions (M = Sc, La, and Y). Once more using a separatory funnel, 10 mL of loaded organic phase was exposed for 10 min to 10 mL of HCl acid solution at various concentrations.

After the aqueous phase was separated, the metal content was determined using an AAS instrument. Fig. 7 presents the stages in a practical manner.

2.6.1. 1Calculating equation

The mass balance equation can be used to compute the M-complex concentration in the organic phases. The following equations were used to calculate the distribution ratio (D), extraction efficiency (E), stripping ratio (S), Caq, which represents the equilibrium concentration of a metal in the stripping solution, and Corg, which represents the initial concentration of a metal in the loaded organic phase:

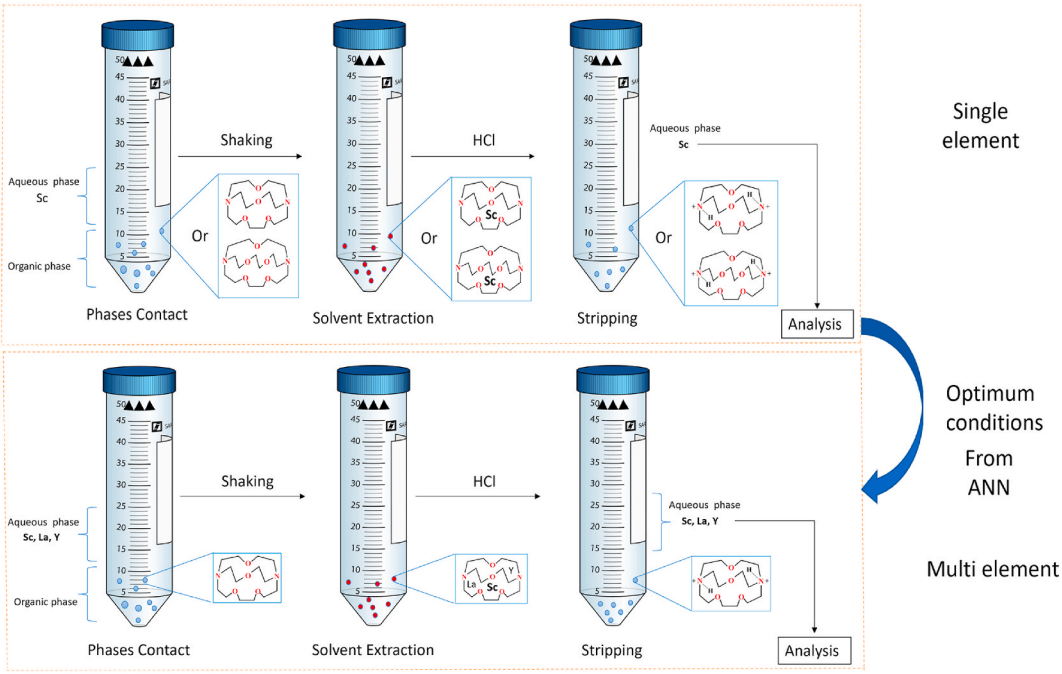

Fig. 7. Schematic representation of extraction and stripping for single and triple-elements model system (Optimum conditions are: organic phase: 0.008 M, A/O: 10 mL:10 mL, shaking time: 10 min, temperature: 25 °C).

$$D_{Sc} = \frac{C_t - C_a}{C_a} \times \frac{V_a}{V_o} \tag{8}$$

where Ct and Ca stand for a metal's initial and ultimate concentrations in water, respectively (ppm).

$$E\,(\%) = \frac{D}{D + \frac{V_a}{V_o}} \times 100 \tag{9}$$

a volume of the organic phase called V_{org} (mL) is a volume of the organic phase (mL); V_{aq} refer to the volume of aqueous phase (mL).

$$S\,(\%) = \frac{C_{aq}}{C_{org}} \times 100 \tag{10}$$

3. Results

3.1. Neural network models performance

ANNs were used to simulate the extraction of Sc ions from an aqueous solution by Cryptand-2.2.1 and Cryptand-2.1.1 using the MATLAB R2021a software. In this study, two different types of neural networks—FFNNs and NARX neural networks—were applied and evaluated for productivity and performance. For the extraction investigation, the best model was utilized to analyze the effects of several parameters, such as pH, concentrations of MCs (mol/L) and Sc (mg/L) and contact time (min).

An ANN-based model was constructed in this study to identify the appropriate parameters for extracting Sc. This was accomplished using a three-layer of FFNNs. The training data was repeated twice (60 data points) to increase the number of data entering the network for the purpose of training and this increases the strength of the network training. However, the data utilized to test the network only consisted of 30 points (Table 4), which were not included in network training. The primary collected data (which contained 60 data points) was subdivided into three subgroups: training, validation, and test. To test the FFNN's ability to recognize "unseen" data that had not been used for testing, the data were divided into subgroups of 70 % for training, 15 % for validation, and 15 % for testing. The generalizability of the FFNNs model can be assessed using this technique. This is the linear regression plot shown in Fig. 8. It shows how the predicted results are compared to the experimental results. If the ANN training is perfect, the network outputs would be exactly the same as the objectives. In reality, it isn't very often that the FFNNs training is so perfect, though.

Even so, it's demonstrated in Fig. 9, the correlation factor (R^2) shows how well measured and predicted values match up. If the R^2 value is one, this means there is a perfect linear relationship between the FFNNs and real-world results. If the R^2 value is near to zero, on the other hand, there is no association between them. As demonstrated in the related figure, the R^2 values for training and testing data in this work are 0.99991 and 0.99991 for C2.2.1 and 0.99994 and 0.99972 for C2.1.1, respectively, indicating an outstanding fit

Table 4
Designed matrix along with observed and predicted response values.

N^0	Experimental variables				Objective function			
					E (%) C 2.2.1		E (%) C 2.1.1	
	MC (mol/L)	pH of Sc solution	Time (min)	Sc (mg/L)	Experimental /observed	Predicted by ANN	Experimental/observed	Predicted by ANN
1	0.008	2	6	100	32	32.70	33	33.00
2	0.006	5	9	75	24	23.91	24.2	24.21
3	0.006	3	9	75	85	83.96	84	84.26
4	0.008	4	12	50	98	99.00	99.3	99.30
5	0.004	2	12	100	18	16.70	17	17.00
6	0.006	3	9	25	97	98.70	99	99.00
7	0.006	3	9	125	60.2	60.70	61	61.00
8	0.008	4	6	100	98	98.70	99	99.00
9	0.004	2	6	50	27	24.72	25	25.02
10	0.004	4	12	100	20	18.70	19	19.00
11	0.008	2	12	50	90	92.69	93	92.99
12	0.006	3	15	75	87	89.70	90	90.00
13	0.002	3	9	75	4.7	4.70	5	5.00
14	0.006	3	9	75	87.3	83.96	87	84.26
15	0.004	4	6	100	19	16.70	17	17.00
16	0.008	4	6	50	99	98.70	99	99.00
17	0.01	3	9	75	99	98.70	99	99.00
18	0.006	1	9	75	15.5	13.70	14	14.00
19	0.004	4	6	50	40	40.70	41	41.00
20	0.004	2	12	50	28	25.72	26	26.02
21	0.008	2	12	100	75	74.90	75.2	75.20
22	0.004	2	6	100	13	10.00	10.3	10.30
23	0.006	3	3	75	70.8	69.71	70	70.01
24	0.004	4	12	50	30	28.71	29	29.01
25	0.008	2	6	50	77	77.70	78	78.00
26	0.008	4	12	100	98	97.71	98	98.01
27	0.006	3	9	75	85	83.96	84	84.26
28	0.006	3	9	75	85	83.96	84	84.26
29	0.006	3	9	75	85	83.96	84	84.26
30	0.006	3	9	75	85	83.96	84	84.26

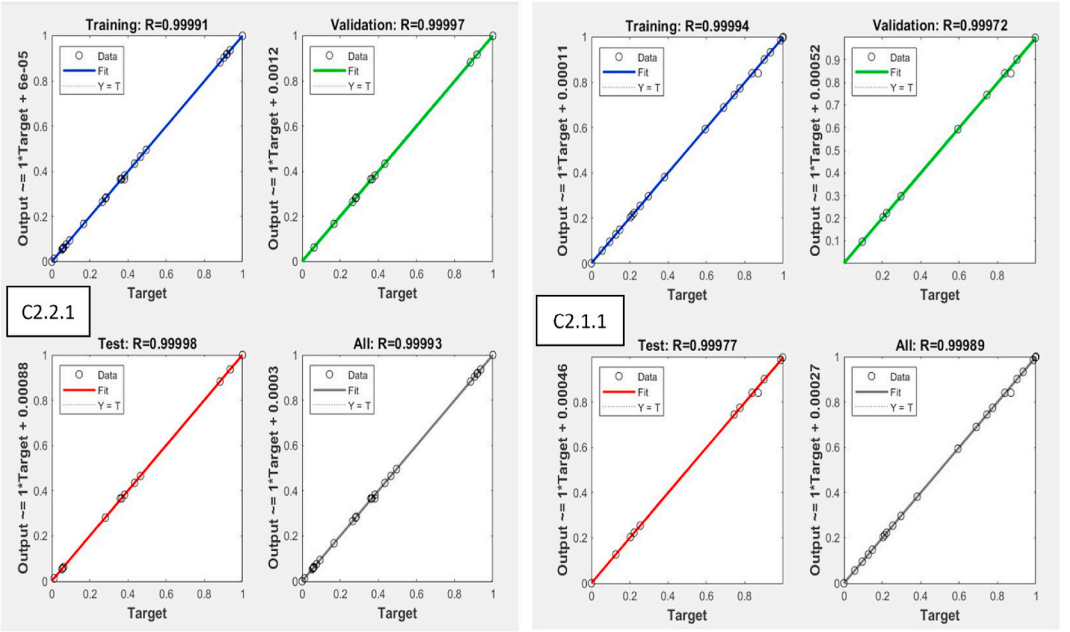

Fig. 8. Results of network design for recovery of Sc–R value of data: (a) train, (b) validation, (c) test, (d) overall.

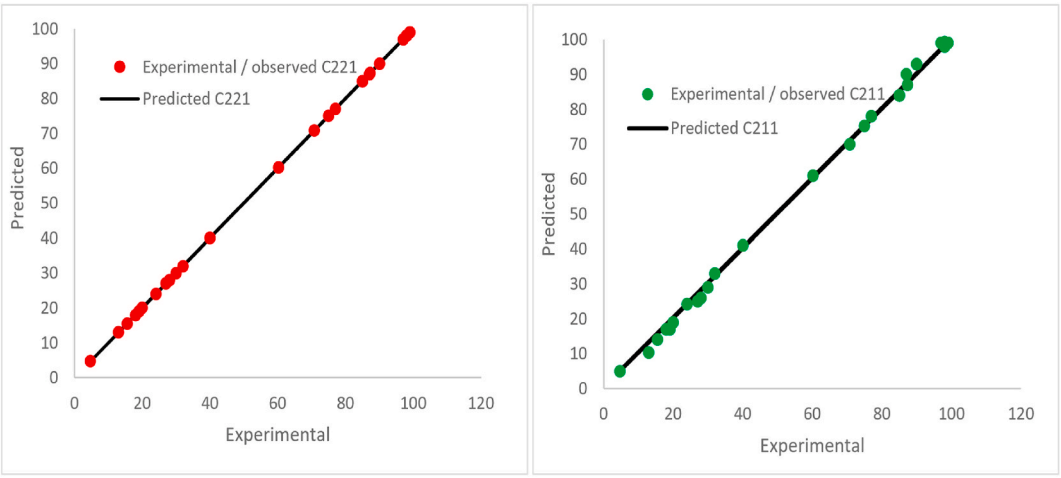

Fig. 9. The actual and predicted values for C2.2.1 and C2.1.1.

between the target data and ANN output. For fresh trials in the validation, preparatory experiments were run using combinations of experimental parameters that weren't in the training data set. Table 4 and Fig. 8(a–d) show the experimental/observed and predicted values. As the number of epochs grows, the MSE of training and testing data lowers, with the highest performance for C2.2.1 and C2.1.1 observed at epochs 3 and 8, respectively, on the validation curve shown in Fig. 10.

The FFNNs model provides the better performance, according to a comparison of the RE and R2 values for the two models. The FFNNs model has an R^2 of 0.9998 and a maximum RE of 12.59% (Fig. 11). It is difficult to choose a model structure with high accuracy and predictability since so many variables must be taken into account, including the number of hidden layers, the neurons in each layer, and the type of transfer function. The optimal network structure in this study was chosen based on network productivity and performance using a variety of node counts, hidden layer configurations, and transfer function types. The performance of the developed neural network model was evaluated based on the testing set using various indicators, using the starting MSE value from the training step; the results are shown in Table 1. The FFNNs model outperformed the NARX model, according to comparisons of the results, which are shown in Fig. 10 for the two models. The numerical values and calculations are presented in Table 5.

3.2. *Recovery of Sc from triple elements solution*

The present optimization results revealed a distinct behavior of the Sc extraction process with two macrocyclic compounds as well as the influence of process operating variables. C 2.1.1 extractant was chosen from the investigated MCs due to its high compatibility (ionic radius ~ 0.8 Å) for the extraction of Sc (ionic radius ~0.7 Å) from triple elements solutions (Sc, La, Y). These elements were chosen for extraction because they have similar physicochemical properties to Sc, although their ionic diameters are different. Consequently, the selectivity of MCs will be indicated.

The following variables were used to conduct the SX investigation of the triple elements system: 25 °C, 0.008 mol/L C 2.1.1 concentration, 10 min of extraction time, 25 mg/L (Sc, La, Y) concentration, and varied starting pH solutions (pH = 2–3). The findings

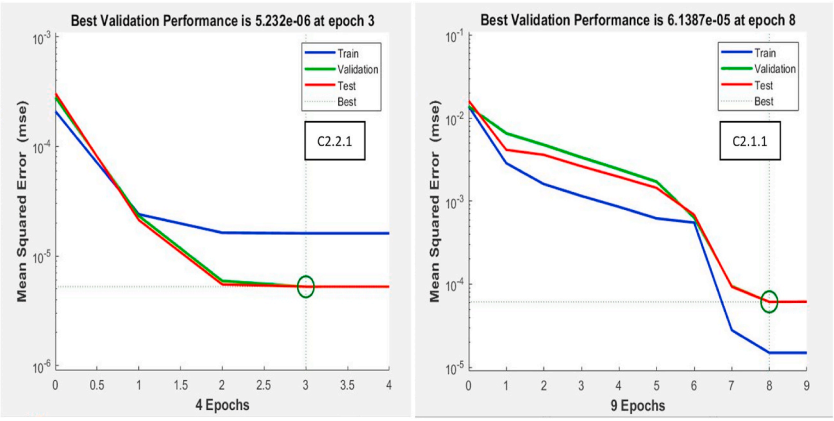

Fig. 10. Performance plot of trained ANN model.

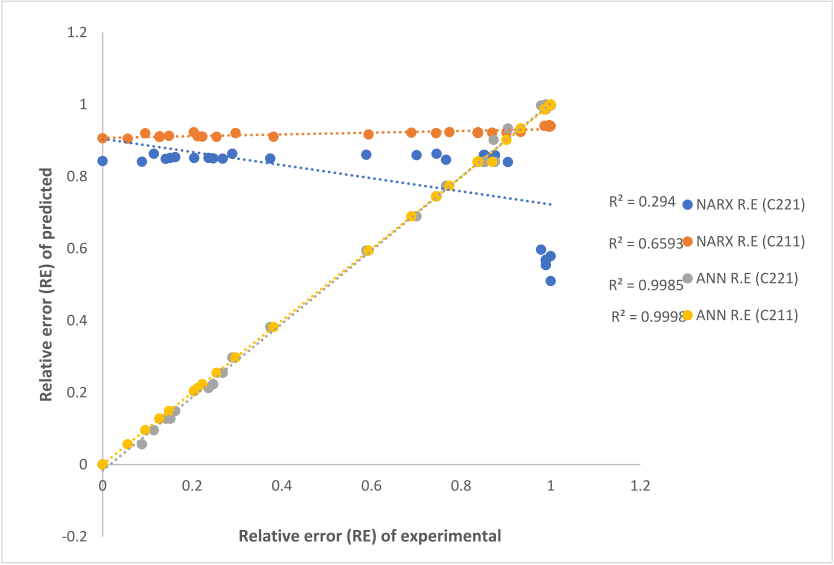

Fig. 11. Coefficients of correlation (R^2) of the neural network models.

Table 5
Initial and final concentration of Sc in single element system.

NO.	MC ,mol/L	pH of Sc solution	Time ,min	Initial concentration Sc ,mg/L	Final concentration Sc ,mg/L by C 2.2.1	E,% C 2.2.1	Final concentration Sc ,mg/L by C 2.1.1	E,% C 2.1.1
1.	0.008	2	6	100	68	32	67	33
2.	0.006	5	9	75	57	24	56	24.2
3.	0.006	3	9	75	11.25	85	12	84
4.	0.008	4	12	50	1	98	0.5	99.3
5.	0.004	2	12	100	82	18	83	17
6.	0.006	3	9	25	0.75	97	0.25	99
7.	0.006	3	9	125	50	60.2	48.75	61
8.	0.008	4	6	100	2	98	1	99
9.	0.004	2	6	50	36.5	27	37.5	25
10.	0.004	4	12	100	80	20	81	19
11.	0.008	2	12	50	5	90	3.5	93
12.	0.006	3	15	75	9.75	87	7.5	90
13.	0.002	3	9	75	71.4	4.7	37.5	5
14.	0.006	3	9	75	9.75	87.3	9.7	87
15.	0.004	4	6	100	81	19	83	17
16.	0.008	4	6	50	0.5	99	0.5	99
17.	0.01	3	9	75	0.75	99	0.75	99
18.	0.006	1	9	75	63.3	15.5	64.5	14
19.	0.004	4	6	50	30	40	29.5	41
20.	0.004	2	12	50	36	28	37	26
21.	0.008	2	12	100	25	75	25.5	75.2
22.	0.004	2	6	100	87	13	89.5	10.3
23.	0.006	3	3	75	22.5	70.8	22.5	70
24.	0.004	4	12	50	35	30	35.5	29
25.	0.008	2	6	50	11.5	77	11	78
26.	0.008	4	12	100	2	98	2	98
27.	0.006	3	9	75	11.25	85	12	84
28.	0.006	3	9	75	11.25	85	12	84
29.	0.006	3	9	75	11.25	85	12	84
30.	0.006	3	9	75	11.25	85	12	84

demonstrated that the initial pH solution value affects the selectivity of C 2.1.1 towered these ions, which have varying ionic radius: Sc~ 0.74 Å, Lã 1.16 Å, and Y~ 0.98 Å [55]. Importantly, the ability of C 2.1.1 to complex and to bind cations in aqueous solutions is particularly sensitive to the pH of the medium since it is a diprotic base. The pH of the solution can be altered to alter binding affinity. At a certain pH level, certain metal ions can bind, and when the pH falls below that level, they can be released [56–58]. By adjusting the pH, it is possible to switch the binding affinity, with metal ion binding taking place at a specific pH and metal ion release occurring at a

lower pH. The C 2.1.1 and C 2.2.1 molecules will be protonated with hydrogen ions from the acid at pH < 1(See Fig. 13), as depicted in Fig. 12. In case of metal complexation, the deprotonation hydrogen ions occur at pH range (2–3). The numerical values and calculations of Sc, Y, La in triple element system are presented in Table 6.

This will make the binding constant for metal cations much lower than that of the neutral C 2.1.1 because of charge repulsion. As shown in Fig. 13, the multielement extraction findings indicated a 99 % selectivity for Sc ions at pH of value 2, compared to 10 % for Y, 7 % for La.

The initial results of recovery studies revealed that the choice of stripping agent and its concentration has a remarkable impact on the selectivity property during the stripping process. The stripping agent used was HCl with a concentration range of 0.1–0.9 mol/L and a step change of 0.2 mol/L, and it was shown that by adjusting the acid concentration, the stripping selectivity could be changed. In terms of interpretation, at 0.1 mol/L HCl acid concentration, Sc achieved 49 % stripping compared to Y 48 %, and La 43 %. At 0.3 mol/L of HCl, Sc was stripped completely from the organic phase, whereas Y was 93 %, La was 91 %. From 0.3 to 0.9 mol/L, the stripping efficiency stayed at high levels as illustrated in Fig. 14. The numerical values and calculations of Sc, Y, La in triple element system are presented in Table 7.

3.3. Extraction Mechanism

It is generally known that metal ions and macrocyclic compounds can create stable complexes. With their 3-D cryptand cavities, cryptate complexes are very stable because of their cation size-cryptand cavity match, and this fit is critical for thermodynamic stability [31,59]. Lanthanides cations, in general, are hard acidic cations that prefer to interact with hard bases like O donor atoms over softer bases like S and P donor atoms [60,61]. Metal complexes with N-donor ligands display some of the most intriguing stoichiometric and practical catalytic changes reported in the scientific literature [62].Because of this, the majority of interactions between neutral ligands and lanthanides cations are conducted by the ligand's donor atoms and these cations. During the cation-MC interaction, the cation is transported from the aqueous phase and held in the cavity of the MC with a weak coordinate covalent bond.

All the previous reports used the synergism extraction system (mixture two or more extractants), a comparison is made between several previously published reports and the current study (Table 8).

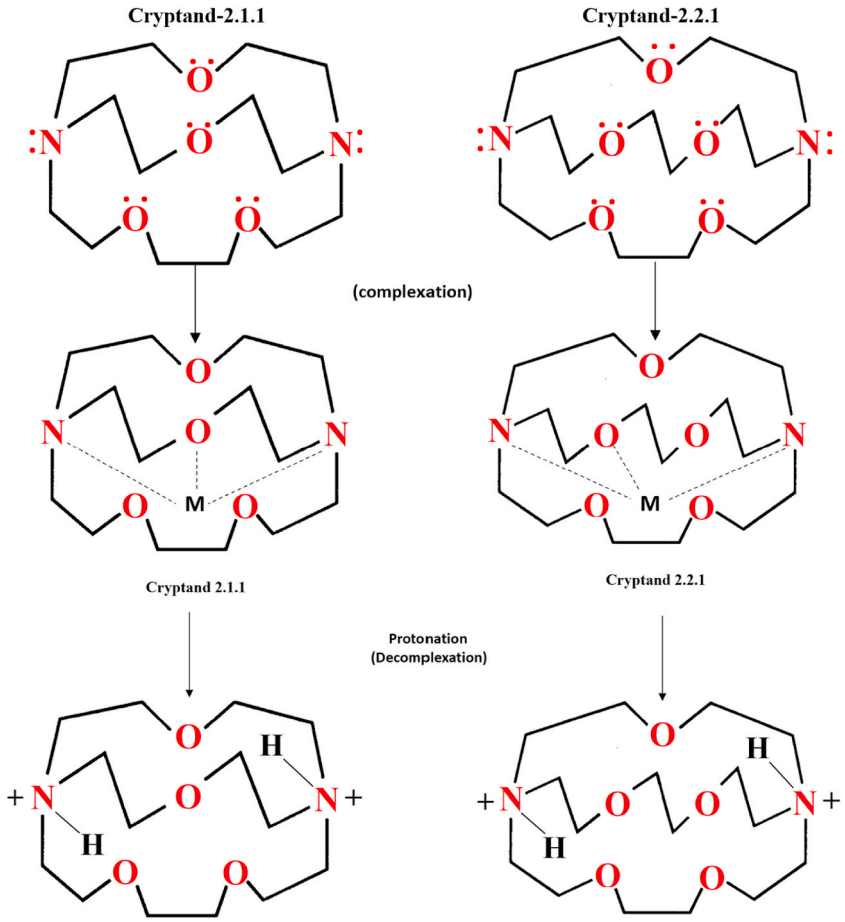

Fig. 12. Schematic representation of complexation and decomplexation of cryptand 2.1.1 and cryptand 2.2.1.

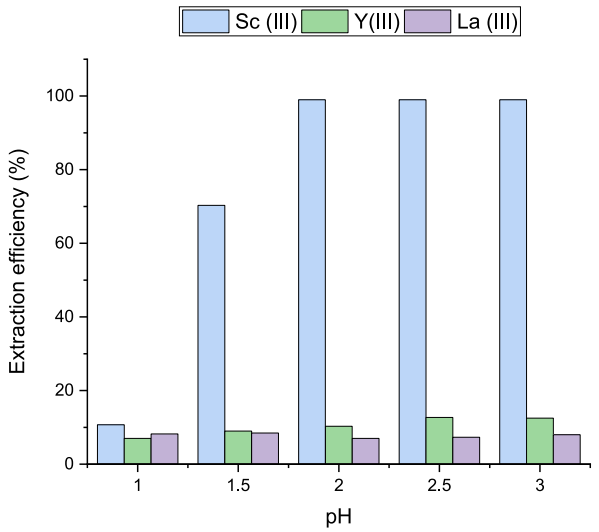

Fig. 13. Extraction experiments of multielement 25 ppm of Sc, La, and Y (organic phase: C2.1.1, A/O: 1, shaking time: 10 min, temperature: 25 °C).

Table 6
Initial and final concentration of Sc, Y, La in triple element system.

Metal ions	Initial concentration, mg/L	Final concentration in aqueous phase, mg/L	Metal ions concentration in organic phase, mg/L	Extraction, %
pH = 1 of triple element solution				
Sc^{3+}	25	22.2	2.8	10.7
Y^{3+}	25	23.2	1.8	7
La^{3+}	25	22.9	2.1	8.2
pH = 1.5 of triple element solution				
Sc^{3+}	25	7.5	17.5	70.3
Y^{3+}	25	22.7	2.3	9
La^{3+}	25	22.9	2.1	8.46
pH = 2 of triple element solution				
Sc^{3+}	25	0.25	24.75	99
Y^{3+}	25	22.4	2.6	10.3
La^{3+}	25	23.25	1.75	7
pH = 2.5 of triple element solution				
Sc^{3+}	25	0.25	24.75	99
Y^{3+}	25	21.8	3.2	12.7
La^{3+}	25	23.1	1.9	7.3
pH = 3 of triple element solution				
Sc^{3+}	25	0.25	24.75	99
Y^{3+}	25	21.8	3.2	12.5
La^{3+}	25	23	2	8

3.4. A comparative study

The comparative study conducted here assessed the performance of the used a nonlinear autoregressive network with exogenous input (NARX) and feed-forward neural network (FFNN) models to estimate their optimum values and compared them with research work that previously utilized other models or one of them. Table 9 presents valuable insights into the effectiveness of these models in enhancing the performance of various processes. The findings indicate that the current study achieves promising results for the scandium recovery process, with a notably high coefficient of determination of 0.999 for two models, surpassing the performance observed in previous studies.

4. Conclusion

This paper investigated the ability and selectivity of C 2.1.1 and C 2.2.1 macrocyclic compounds as novel extractants for Sc from the nitric acid medium. The Artificial Neural Network (ANN) was found to be effective tool for determining the optimal conditions for Sc extraction in a variety of operating parameters. Based on a comparison of the performance and accuracy of the NARX and FFNN models, it was found that the FFNN model performed better than the NARX model. Maximum RE for the FFNN model was 12.59%, R^2 was 0.9998, and MSE for C221 and C211 were 5.232*10-6 and 6.1387*10-5, respectively.

The modeling was performed using 30 experimental data points corresponding to various operating parameters such as MC

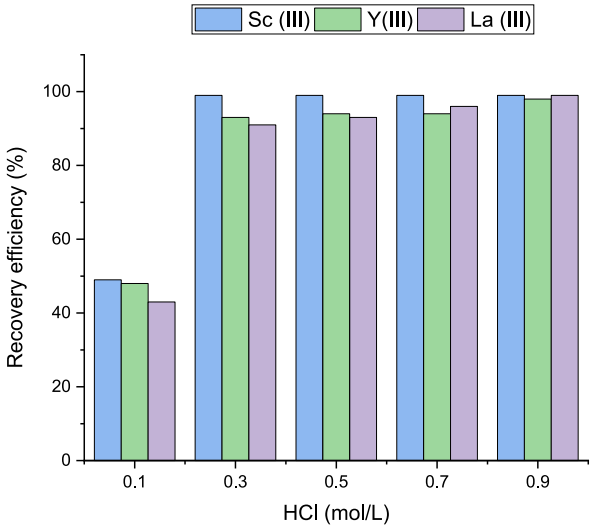

Fig. 14. Recovery experiments of multielement from 25 ppm Sc, La, and Y (organic phase: C2.1.1, A/O: 1, shaking time: 10 min, temperature: 25 °C).

Table 7
The effect of hydrochloric acid, stripping agent concentration on metal ions recovery efficiency (organic phase: C2.1.1, A/O: 1, shaking time: 10 min, temperature: 25 °C, pH of extraction:2).

Metal ions	Metal ions concentration in organic phase, mg/L	Concentration of HCl, mol/L	Final concentration in aqueous phase, mg/L	Recovery, %
Sc^{3+}	24.75	0.1	12.12	49
Y^{3+}	2.6		1.24	48
La^{3+}	1.75		0.75	43
Sc^{3+}	24.75	0.3	24.5	99
Y^{3+}	2.6		2.4	93
La^{3+}	1.75		1.5	91
Sc^{3+}	24.75	0.5	24.50	99
Y^{3+}	2.6		2.44	94
La^{3+}	1.75		1.62	93
Sc^{3+}	24.75	0.7	24.4	99
Y^{3+}	2.6		2.4	94
La^{3+}	1.75		1.68	96
Sc^{3+}	24.75	0.9	24.5	99
Y^{3+}	2.6		2.54	98
La^{3+}	1.75		1.73	99

concentration, pH, contact time, and Sc concentration. In order to predict the optimum conditions for Sc extraction, a three-layer back propagation model with multiple training functions in the hidden and output layers was used in conjunction with non-linear regression. Two performance metrics were used to evaluate models: MSE and coefficient of determination (R^2), which were then validated using additional datasets. According to the extraction studies, the ideal conditions for MC extractants to achieve 99% Sc extraction efficiency are as follows: pH 2 of the aqueous solution, 0.008 mol/L MC concentration, and an initial Sc concentration of 75 mg/L. The predicted conditions based on the results of ANN were applied for extracting Sc from the multielement matrix (Sc, La, Y). Based on the optimum conditions from ANN, Sc was extracted from a multielement solution (Sc, Y, La). Additionally, it was discovered during the recovery research that the concentration and kind of stripping agent have a considerable impact on selectivity. As a result, the extraction of Sc was 99% at a concentration of 0.3 mol/L of HCl acid as opposed to 10% for Y and 7% for La.

Data availability

All data generated or analyzed during this study are included in this published article.

Ethics approval and consent to participate

Not applicable.

Table 8
Comparison of solvent extraction techniques for Sc recovery.

Extraction step		Stripping step		Extracted element	Year/References
Extractant	E, %	Stripping agent	S,%		
15 % D2EHPA 5 % TBP	99.00	2 M NaOH	95.40	Sc	(2017) [26]
8 % D2EHPA 2 % TBP	99.70	2 M NaOH +1 M NaCl	85.00	Sc	(2018) [63]
16 % D2EHPA 4 % TBP	99.00	2 M NaOH	96.00	Sc	(2019) [64]
60 % Cyanex272 40 % Cyanex923	98.00	10 % $H_2C_2O_4$	98.80	Sc	(2020) [65]
15 % D2EHPA 15 % N1923	99.00	5 M HNO_3	89.30	Sc	(2020) [66]
10 % D2EHPA 5 % TBP	99.00	5 M NaOH	99.61	Sc	(2021) [67]
10 % D2EHPA 5 % TBP	99.00	3 M NaOH	99.00	Sc	(2021) [68]
10 % Cyanex 923 10 % Alamine336	92 %	5 M H_3PO_4	100 %	Sc, Zr	(2021) [69]
0.05 M D2EHPA	97 %	2.5 M NaOH	95.00	Sc, Fe	(2022) [8]
12.5 % TBP	99 %	1 M HCl	92.85	Sc, Fe	

Note: all the tabulated percentages in this table were calculated based on the organic phase.

Table 9
Comparative study that applied artificial neural network models.

No.	Input	Output or response	Type of ions uptake or removed	Mathematical model type	R^2	Ref.
1	initial concentration, adsorbent dosage, and pH	Removal efficiency	Nickel (Ni)	ANN	0.98	[70]
2	adsorbent dosage, contact time, Hg concentration and pH	Removal efficiency	Mercury (Hg)	FFNNs	0.97	[54]
3	pH, contact time adsorbent dosages and initial Cd^{2+} concentrations	Removal efficiency	Cadmium (Ca^{+2})	ANN	0.99	[71]
4	concentration of MC, concentration of Sc, pH, and time	Recovery efficiency	scandium (Sc)	FFNNs and NARX neural networks	0.999	This study

Consent for publication

Not applicable.

CRediT authorship contribution statement

Ali Dawood Salman: Conceptualization, Data curation, Investigation, Methodology, Resources, Validation, Writing – original draft, Writing – review & editing. **Saja Mohsen Alardhi:** Data curation, Investigation, Methodology, Software, Validation, Visualization, Writing – original draft. **Forat Yasir AlJaberi:** Formal analysis, Investigation, Resources, Validation. **Moayyed G. Jalhoom:** Conceptualization, Formal analysis, Methodology, Validation. **Phuoc-Cuong Le:** Project administration, Resources, Supervision. **Shurooq Talib Al-Humairi:** Investigation, Software, Validation. **Mohammademad Adelikhah:** Formal analysis, Resources, Visualization. **Miklós Jakab:** Formal analysis, Investigation, Resources. **Gergely Farkas:** Resources, Software. **Alaa Abdulhady Jaber:** Formal analysis, Validation, Visualization.

Declaration of competing interest

The authors declare that they have no known competing financial interests or personal relationships that could have appeared to influence the work reported in this paper.

Acknowledgment

This work was supported by the Ministry of Education and Training of Vietnam with project (B2022-DNA-04) for their generous support of this research.

References

[1] A.B. Botelho Junior, D.C.R. Espinosa, J. Vaughan, J.A.S. Tenório, Recovery of scandium from various sources: a critical review of the state of the art and future prospects, Miner. Eng. 172 (2021), 107148, https://doi.org/10.1016/j.mineng.2021.107148.

[2] A.D. Salman, T. Juzsakova, R. Ákos, R.I. Ibrahim, M.A. Al-Mayyahi, S. Mohsen, T.A. Abdullah, E. Domokos, Synthesis and surface modification of magnetic Fe3O4@SiO2 core-shell nanoparticles and its application in uptake of scandium (III) ions from aqueous media, Environ. Sci. Pollut. Control Ser. 28 (22) (2021) 28428–28443, https://doi.org/10.1007/s11356-020-12170-4.

[3] D. Zou, Y. Deng, J. Chen, D. Li, A review on solvent extraction of scandium, J. Rare Earths (2022), https://doi.org/10.1016/j.jre.2021.12.009.

[4] G. Li, Q. Ye, B. Deng, J. Luo, M. Rao, Z. Peng, T. Jiang, Extraction of scandium from scandium-rich material derived from bauxite ore residues, Hydrometallurgy 176 (2018) 62–68.

[5] Q. Yu, S. Ning, W. Zhang, X. Wang, Y. Wei, Recovery of scandium from sulfuric acid solution with a macro porous TRPO/SiO2-P adsorbent, Hydrometallurgy 181 (2018) 74–81.

[6] N. Zhang, H.-X. Li, X.-M. Liu, Recovery of scandium from bauxite residue—red mud: a review, Rare Met. 35 (12) (2016) 887–900.

[7] A.D. Salman, T. Juzsakova, S. Mohsen, T.A. Abdullah, P.-C. Le, V. Sebestyen, B. Sluser, I. Cretescu, Scandium recovery methods from mining, Metallurgical Extractive Industries, and Industrial Wastes, Materials 15 (7) (2022) 2376.

[8] A.D. Salman, T. Juzsakova, M.G. Jalhoom, T.A. Abdullah, P.-C. Le, S. Viktor, E. Domokos, X.C. Nguyen, D.D. La, A.K. Nadda, D.D. Nguyen, A selective hydrometallurgical method for scandium recovery from a real red mud leachate: a comparative study, Environ. Pollut. 308 (2022), 119596, https://doi.org/10.1016/j.envpol.2022.119596.

[9] C. Liu, L. Chen, J. Chen, D. Zou, Y. Deng, D. Li, Application of P507 and isooctanol extraction system in recovery of scandium from simulated red mud leach solution, J. Rare Earths 37 (9) (2019) 1002–1008.

[10] W. Wang, Y. Pranolo, C.Y. Cheng, Metallurgical processes for scandium recovery from various resources: a review, Hydrometallurgy 108 (1) (2011) 100–108, https://doi.org/10.1016/j.hydromet.2011.03.001.

[11] C.R. Borra, B. Blanpain, Y. Pontikes, K. Binnemans, T. Van Gerven, Recovery of rare earths and other valuable metals from bauxite residue (red mud): a review, Journal of Sustainable Metallurgy 2 (4) (2016) 365–386.

[12] B. Onghena, K. Binnemans, Recovery of scandium(III) from aqueous solutions by solvent extraction with the functionalized ionic liquid betainium bis (trifluoromethylsulfonyl)imide, Ind. Eng. Chem. Res. 54 (6) (2015) 1887–1898, https://doi.org/10.1021/ie504765v.

[13] B. Onghena, C.R. Borra, T. Van Gerven, K. Binnemans, Recovery of scandium from sulfation-roasted leachates of bauxite residue by solvent extraction with the ionic liquid betainium bis(trifluoromethylsulfonyl)imide, Sep. Purif. Technol. 176 (2017) 208–219, https://doi.org/10.1016/j.seppur.2016.12.009.

[14] R.P. Narayanan, L.-C. Ma, N.K. Kazantzis, M.H. Emmert, Cost analysis as a tool for the development of Sc recovery processes from bauxite residue (red mud), ACS Sustain. Chem. Eng. 6 (4) (2018) 5333–5341.

[15] C. Wang, D. Li, EXTRACTION MECHANISM OF Sc (III) AND SEPARATION FROM ThUV). Fe (III) AND Lu (III) WITH BIS (2, 4, 4-TRIMETHYLPENTYL) PHOSPHINIC ACID IN N-HEXANE FROM SULPHURIC ACID SOLUTIONS, Solvent Extr. Ion Exch. 12 (3) (1994) 615–631.

[16] Y. Zhang, H. Zhao, M. Sun, Y. Zhang, X. Meng, L. Zhang, X. Lv, S. Davaasambuu, G. Qiu, Scandium extraction from silicates by hydrometallurgical process at normal pressure and temperature, J. Mater. Res. Technol. 9 (1) (2020) 709–717, https://doi.org/10.1016/j.jmrt.2019.11.012.

[17] Ş. Kaya, Y.A. Topkaya, Chapter 11 - extraction behavior of scandium from a refractory nickel laterite ore during the pressure acid leaching process, in: I. Borges De Lima, W. Leal Filho (Eds.), Rare Earths Industry, Elsevier, Boston, 2016, pp. 171–182, https://doi.org/10.1016/B978-0-12-802328-0.00011-5.

[18] J. Shibata, N. Murayama, Solvent extraction of scandium from the waste solution of TiO2 production process, Trans. Indian Inst. Met. 70 (2) (2017) 471–477, https://doi.org/10.1007/s12666-016-1008-3.

[19] A.D. Salman, T. Juzsakova, Á. Rédey, P.-C. Le, X.C. Nguyen, E. Domokos, T.A. Abdullah, V. Vagvolgyi, S.W. Chang, D.D. Nguyen, Enhancing the recovery of rare earth elements from red mud, Chem. Eng. Technol. 44 (10) (2021) 1768–1774, https://doi.org/10.1002/ceat.202100223.

[20] X.-j. Wang, X.-k. Li, Scandium Extraction from Red Mud Solution by Emulsion Liquid Membrane, Nonferrous Metals (Extractive Metallurgy), 2008.

[21] A.D. Salman, T. Juzsakova, M.G. Jalhoom, P.-C. Le, T.A. Abdullah, I. Cretescu, E. Domokos, V.-H. Nguyen, Potential application of macrocyclic compounds for selective recovery of rare earth scandium elements from aqueous media, Journal of Sustainable Metallurgy (2022), https://doi.org/10.1007/s40831-021-00484-7.

[22] W. Yoshida, Y. Baba, F. Kubota, S.D. Kolev, M. Goto, Selective transport of scandium(III) across polymer inclusion membranes with improved stability which contain an amic acid carrier, J. Membr. Sci. 572 (2019) 291–299, https://doi.org/10.1016/j.memsci.2018.11.021.

[23] N.K. Batchu, Z. Li, B. Verbelen, K. Binnemans, Structural effects of neutral organophosphorus extractants on solvent extraction of rare-earth elements from aqueous and non-aqueous nitrate solutions, Sep. Purif. Technol. 255 (2021), 117711, https://doi.org/10.1016/j.seppur.2020.117711.

[24] D. Flett, Solvent extraction in hydrometallurgy: the role of organophosphorus extractants, Journal of Organometallic Chemistry - J ORGANOMET CHEM 690 (2005) 2426–2438, https://doi.org/10.1016/j.jorganchem.2004.11.037.

[25] W. Zhang, T.-A. Zhang, G. Lv, W. Zhou, X. Cao, H. Zhu, Extraction separation of Sc (III) and Fe (III) from a strongly acidic and highly concentrated ferric solution by D2EHPA/TBP, Jom 70 (12) (2018) 2837–2845.

[26] X. Zhu, W. Li, S. Tang, M. Zeng, P. Bai, L. Chen, Selective recovery of vanadium and scandium by ion exchange with D201 and solvent extraction using P507 from hydrochloric acid leaching solution of red mud, Chemosphere 175 (2017) 365–372.

[27] L. Fabbrizzi, The origins of the coordination chemistry of alkali metal ions, ChemTexts 6 (2) (2020) 1–19.

[28] X.X. Zhang, R.M. Izatt, J.S. Bradshaw, K.E. Krakowiak, Approaches to improvement of metal ion selectivity by cryptands, Coord. Chem. Rev. 174 (1) (1998) 179–189.

[29] D. Bandyopadhyay, Crowns and crypts, Resonance 6 (2001) 71–79, https://doi.org/10.1007/BF02907367.

[30] R.L. Sundberg, Crown ethers: applications in inorganic synthesis, Senior Scholar Papers (1978) 232.

[31] S.K. Menon, S.V. Hirpara, U. Harikrishnan, Synthesis and applications of cryptands, Rev. Anal. Chem. 23 (4) (2004) 233–268.

[32] A. Salman, T. Juzsakova, M. Jalhoom, R. Ibrahim, E. Domokos, M. Al-Mayyahi, T. Abdullah, B. Szabolcs, S. Al-Nuzal, Studying the extraction of scandium (III) by macrocyclic compounds from aqueous solution using optimization technique, Int. J. Environ. Sci. Technol. (2022) 1–18.

[33] A.D. Salman, T. Juzsakova, M.G. Jalhoom, C. Le Phuoc, S. Mohsen, T. Adnan Abdullah, B. Zsirka, I. Cretescu, E. Domokos, C.D. Stan, Novel hybrid nanoparticles: synthesis, functionalization, characterization, and their application in the uptake of scandium (III) ions from aqueous media, Materials 13 (24) (2020) 5727.

[34] M.A. Jasim, F.Y. AlJaberi, A.D. Salman, S.M. Alardhi, P.-C. Le, G. Kulcsár, M. Jakab, Studying the effect of reactor design on the electrocoagulation treatment performance of oily wastewater, Heliyon 9 (7) (2023), e17794, https://doi.org/10.1016/j.heliyon.2023.e17794.

[35] S.S. Fiyadh, S.M. Alardhi, M. Al Omar, M.M. Aljumaily, M.A. Al Saadi, S.S. Fayaed, S.N. Ahmed, A.D. Salman, A.H. Abdalsalm, N.M. Jabbar, A. El-Shafi, A comprehensive review on modelling the adsorption process for heavy metal removal from waste water using artificial neural network technique, Heliyon 9 (4) (2023), e15455, https://doi.org/10.1016/j.heliyon.2023.e15455.

[36] S.M. Alardhi, A.H. Abdalsalam, A.A. Ati, M.H. Abdulkareem, A.A. Ramadhan, M.M. Taki, Z.Y. Abbas, Fabrication of polyaniline/zinc oxide nanocomposites: synthesis, characterization and adsorption of methylene orange, Polym. Bull. (2023), https://doi.org/10.1007/s00289-023-04753-1.

[37] N.M. Jabbar, S.M. Alardhi, T. Al-Jadir, H. Abed Dhahad, Contaminants removal from real refinery wastewater associated with energy generation in microbial fuel cell, J. Ecol. Eng. 24 (1) (2023) 107–114, https://doi.org/10.12911/22998993/156081.

[38] S.M. Alardhi, F.Y. Aljaberi, W.A. Kadhim, T.A.- Jadir, L.M. Alsaedi, N.M. Jabbar, A. Almarmadh, G.G. Komsh, M. Adnan, Investigating the capability of MCM-41 nanoparticle for COD removal from Iraqi petroleum refinery wastewater, AIP Conf. Proc. 2820 (1) (2023), https://doi.org/10.1063/5.0151096.

[39] Z.U. Ahmad, L. Yao, Q. Lian, F. Islam, M.E. Zappi, D.D. Gang, The use of artificial neural network (ANN) for modeling adsorption of sunset yellow onto neodymium modified ordered mesoporous carbon, Chemosphere 256 (2020), 127081, https://doi.org/10.1016/j.chemosphere.2020.127081.

[40] N. Gammoudi, M. Mabrouk, T. Bouhemda, K. Nagaz, A. Ferchichi, Modeling and optimization of capsaicin extraction from Capsicum annuum L. using response surface methodology (RSM), artificial neural network (ANN), and Simulink simulation, Ind. Crop. Prod. 171 (2021), 113869, https://doi.org/10.1016/j.indcrop.2021.113869.

[41] C. Hu, S. Fu, L. Zhu, W. Dang, T. Zhang, Evaluation and prediction on the effect of ionic properties of solvent extraction performance of oily sludge using machine learning, Molecules 26 (24) (2021) 7551.

[42] S.M. Alardhi, N.M. Jabbar, T. AL-Jadir, N.K. Ibrahim, A.M. Dakhil, N.D. Al-Saedi, H.D. Al-Saedi, M. Adnan, Artificial neural network model for predicting the desulfurization efficiency of Al-Ahdab crude oil, AIP Conf. Proc. 2443 (1) (2022), 030033, https://doi.org/10.1063/5.0091975.

[43] S.M. Alardhi, T. Al-Jadir, A.M. Hasan, A.A. Jaber, L.M. Al Saedi, Design of artificial neural network for prediction of hydrogen sulfide and carbon dioxide concentrations in a natural gas sweetening plant, Ecological Engineering & Environmental Technology 24 (2) (2023) 55–66, https://doi.org/10.12912/27197050/157092.

[44] Artificial neural networks in hydrology. I: preliminary concepts, J. Hydrol. Eng. 5 (2) (2000) 115–123.

[45] E. Grossi, M. Buscema, Introduction to artificial neural networks, Eur. J. Gastroenterol. Hepatol. 19 (2008) 1046–1054, https://doi.org/10.1097/MEG.0b013e3282f198a0.

[46] S.M. Alardhi, S.S. Fiyadh, A.D. Salman, M. Adelikhah, Prediction of methyl orange dye (MO) adsorption using activated carbon with an artificial neural network optimization modeling, Heliyon (2023), e12888, https://doi.org/10.1016/j.heliyon.2023.e12888.

[47] T. Aung, S.-J. Kim, J.-B. Eun, A hybrid RSM-ANN-GA approach on optimisation of extraction conditions for bioactive component-rich laver (Porphyra dentata) extract, Food Chem. 366 (2022), 130689.

[48] T. Al-Jadir, S.M. Alardhi, F. Al-Sheikh, A.A. Jaber, W.A. Kadhim, M.H.A. Rahim, Modeling of lead (II) ion adsorption on multiwall carbon nanotubes using artificial neural network and Monte Carlo technique, Chem. Eng. Commun. (2022) 1–17, https://doi.org/10.1080/00986445.2022.2129622.

[49] R.S. Govindaraju, Artificial neural networks in hydrology. I: preliminary concepts, J. Hydrol. Eng. 5 (2) (2000) 115–123.

[50] A.H. Mahdi, G.M. Jaid, S.M. Alardhi, Artificial neural network modelling for the removal of lead from wastewater by using adsorption process, Desalination Water Treat. 244 (2021) 110–119.

[51] E.H. Flaieh, F.O. Hamdoon, A.A. Jaber, Estimation the natural frequencies of a cracked shaft based on finite element modeling and artificial neural network, Int. J. Adv. Sci. Eng. Inf. Technol. 10 (2020) 1410–1416.

[52] A.A. Jaber, A.A. Saleh, H.F.M. Ali, Prediction of hourly cooling energy consumption of educational buildings using artificial neural network, Space 10137 (2019) m3.

[53] S. Chen, S. Billings, P. Grant, Non-linear system identification using neural networks, Int. J. Control 51 (6) (1990) 1191–1214.

[54] S.S. Fiyadh, M.K. AlOmar, W.Z. Binti Jaafar, M.A. AlSaadi, S.S. Fayaed, S. Binti Koting, S.H. Lai, M.F. Chow, A.N. Ahmed, A. El-Shafie, Artificial neural network approach for modelling of mercury ions removal from water using functionalized CNTs with deep eutectic solvent, Int. J. Mol. Sci. 20 (17) (2019) 4206.

[55] W.H. Wells, V.L. Wells, The Lanthanides, Rare Earth Elements, Patty's Toxicology, pp. 817-840. https://doi.org/https://doi.org/10.1002/0471435139.tox043.pub2.

[56] G. Alibrandi, Cryptand 111: a chemical device for variable-pH kinetic experiments, Angew. Chem. 47 (2008) 3026–3028, https://doi.org/10.1002/anie.200800180.

[57] M.N. Gandhi, S.M. Khopkar, Liquid-liquid extraction of copper(II) with cryptand 222 with erythrosine B as the counter-ion, Microchim. Acta 111 (1) (1993) 93–101, https://doi.org/10.1007/BF01240171.

[58] H. Luo, S. Dai, P. Bonnesen, Solvent extraction of Sr 2+ and Cs + based on room-temperature ionic liquids containing monoaza-substituted crown ethers, Analytical chemistry 76 (2004) 2773–2779, https://doi.org/10.1021/ac035473d.

[59] E. Leite, S. Santana, P. Hünenberger, L. Freitas, R. Longo, On the relative stabilities of the alkali cations 222 cryptates in the gas phase and in water-methanol solution, J. Mol. Model. 13 (2007) 1017–1025, https://doi.org/10.1007/s00894-007-0213-8.

[60] N.P. Bessen, I.A. Popov, C.R. Heathman, T.S. Grimes, P.R. Zalupski, L.M. Moreau, K.F. Smith, C.H. Booth, R.J. Abergel, E.R. Batista, P. Yang, J.C. Shafer, Complexation of lanthanides and heavy actinides with aqueous sulfur-donating ligands, Inorg. Chem. 60 (9) (2021) 6125–6134, https://doi.org/10.1021/acs.inorgchem.1c00257.

[61] K.L. Haas, K.J. Franz, Application of metal coordination chemistry to explore and manipulate cell biology, Chem Rev 109 (10) (2009) 4921–4960, https://doi.org/10.1021/cr900134a.

[62] Q. Shi, R.J. Thatcher, J. Slattery, P.S. Sauari, A.C. Whitwood, P.C. McGowan, R.E. Douthwaite, Synthesis, coordination chemistry and bonding of strong N-donor ligands incorporating the 1H-Pyridin-(2E)-Ylidene (PYE) motif, Chem. Eur J. 15 (42) (2009) 11346–11360, https://doi.org/10.1002/chem.200901382.

[63] W. Zhang, T.-A. Zhang, G. Lv, W. Zhou, X. Cao, H. Zhu, Extraction separation of Sc(III) and Fe(III) from a strongly acidic and highly concentrated ferric solution by D2EHPA/TBP, JOM 70 (12) (2018) 2837–2845, https://doi.org/10.1007/s11837-018-3166-8.

[64] H. Qiu, M. Wang, Y. Xie, J. Song, T. Huang, X.-M. Li, T. He, From trace to pure: recovery of scandium from the waste acid of titanium pigment production by solvent extraction, Process Saf. Environ. Protect. 121 (2019) 118–124.

[65] J. Hu, D. Zou, J. Chen, D. Li, A novel synergistic extraction system for the recovery of scandium (III) by Cyanex272 and Cyanex923 in sulfuric acid medium, Sep. Purif. Technol. 233 (2020), 115977, https://doi.org/10.1016/j.seppur.2019.115977.

[66] D. Zou, H. Li, J. Chen, D. Li, Recovery of scandium from spent sulfuric acid solution in titanium dioxide production using synergistic solvent extraction with D2EHPA and primary amine N1923, Hydrometallurgy 197 (2020), 105463.

[67] Y. Chen, S. Ma, S. Ning, Y. Zhong, X. Wang, T. Fujita, Y. Wei, Highly efficient recovery and purification of scandium from the waste sulfuric acid solution from titanium dioxide production by solvent extraction, J. Environ. Chem. Eng. 9 (5) (2021), 106226.

[68] J. Zhou, S. Ma, Y. Chen, S. Ning, Y. Wei, T. Fujita, Recovery of scandium from red mud by leaching with titanium white waste acid and solvent extraction with P204, Hydrometallurgy 204 (2021), 105724.

[69] A.B. Botelho Junior, D.C.R. Espinosa, J.A.S. Tenório, Selective separation of Sc(III) and Zr(IV) from the leaching of bauxite residue using trialkylphosphine acids, tertiary amine, tri-butyl phosphate and their mixtures, Sep. Purif. Technol. 279 (2021), 119798, https://doi.org/10.1016/j.seppur.2021.119798.

[70] B. Mehdi, D. Brahmi-Ingrachen, H. Belkacemi, L. Muhr, Development of a mathematical model based on an artificial neural network (ANN) to predict nickel uptake data by a natural zeolite, Physical Sciences Forum 6 (1) (2023) 4.

[71] A. Takdastan, S. Samarbaf, Y. Tahmasebi, N. Alavi, A.A. Babaei, Alkali modified oak waste residues as a cost-effective adsorbent for enhanced removal of cadmium from water: isotherm, kinetic, thermodynamic and artificial neural network modeling, J. Ind. Eng. Chem. 78 (2019) 352–363, https://doi.org/10.1016/j.jiec.2019.05.034.